

Dear reviewers,

Thank you so much for your feedback and for taking the time to review this article.

We have replied to your comments below. We will further work on trying to reduce the length of the paper and perform a thorough proofreading before submitting a revised version.

Again, we appreciate your time,

Emmanuel, Dylan and Cameron

Reviewer 1:

The subject is relevant and important, namely the estimation of turbine loads in real time. It is generally considered true that manufacturers are aiming to make their turbines smarter and this includes such technology. However, the abstract mentions real-time fatigue life consumption specifically, and it is this reviewer's opinion that no one needs to know fatigue life consumption in real-time. Perhaps other uses of real-time load estimation could help readers see the importance of the work.

>>> Thank you for this useful comment. We have added that the method can also be applied to condition monitoring, or to develop dedicated control strategies.

The method is broadly applicable, to most turbine types onshore, with a discussion about the future offshore. The techniques used are explained well and are well understood by engineers in this field. The validation method is good and honest - too often signal estimation is claimed to absurd accuracy. The conclusions accurately represent the body of the work. The language used is appropriate, not being too heavy on mathematics that only mathematicians would know. Important areas of nuance and difficulty are expounded, rather than glossed over, which is refreshing. The paper could be shorter, but possibly at the expense of reproducibility by future readers. The references are relevant and cover the field reasonably well. It could be said that there are interesting load estimators that do not require KF, but perhaps the author wants to focus only on KF.

>>> We are indeed only focusing on KF methods, but to address your comments, we have now mentioned this limitation and added some references to other load estimation techniques (such as lookup table, machine learning, or modal expansion)

Proofreading notes:

* Line 18 "Wind turbines are designed and optimized for a given site" - or are they designed to a class definition?

>>> This is a fair point. We've added "class definition" in the sentence since site-specific (or position-specific) designs might not be the norm yet.

* Line 42 has a citation to "M." - unless this is James Bond's boss, this might be a Latex error.

>>> Thank you for noticing this and thank you for using humor!

* Line 49 talks about fatigue life consumption of "turbine components" - there is a huge variety in methods of FLC, so since this paper is only about rainflow counting for the tower, perhaps reword this to be less overreaching?

>>> The sentence now precise that rainflow counting is used, and the only component considered in this study is the tower.

* Line 55 makes it sound like thrust is all you need for the loads up the tower. Isn't rotor asymmetric loading from e.g. shear more significant as you go up the tower?

>>> Yes, it is true, the tilt and yaw loads will not be captured with only a tower top accelerometer. Yaw loads generate torsion on the tower so they are not so important for tower fatigue monitoring. But tilt loads add to the bending moment. Tilt moments are constant down the tower but thrust induced moments increase as you go down with the moment arm length. So the relative importance between tilt loading and thrust loading varies through the tower. At the tower bottom the tilt loads are pretty much insignificant contributor but at the tower top they are the main contributor. So the fatigue loads on the top part (e.g. 20-30%) of the tower would not be accurately estimated with the simple model presented in the paper. We added the following to the introduction "It is noted that the method is expected to be more accurate at the tower-bottom than the tower-top since rotor asymmetric loading is not captured."

* Line 160 inline equation $X_{\{x_d\}}$ I think should be $X_{\{x,d\}}$.

* Line 186 "where ρ " should be after equation (13) not (14)

* Line 199 another citation error to WG3?

* Line 355 previously you have amounts of time in the main text, not math mode so this time constant of 1s looks odd with the s italic.

>>> Thank you for noticing these errors, they have now been corrected.

Reviewer 2:

This paper presents:

*An application of the Kalman filtering technique to estimate tower-base loads on a wind turbine using readily available measurements and a simple 2-DOF model, e.g., for use as a digital twin.

*Validation of the method using OpenFAST simulations for a land-based wind turbine.

*Recommendations for future work in this area.

Overall, the paper is well written, the results appear to be scientifically sound, and the results are informative. A few corrections and clarifications are warranted to approve the final publication. Please find specific comments and technical corrections below:

Specific Comments (Page / Line / Comment):

3 / 67 / Do the stiffness and damping account for aerodynamic stiffness and damping, or just structural? I.e. do the aero- dynamic stiffness and damping come from T_a^* or through C and K.
>> Thank you for this comment, we have now added some precision in the text. The damping C has been tuned to account for aerodynamic damping (using a decay test with the turbine operating). This damping is currently assumed to hold for all wind speeds, which is a rough approximation. The aerodynamic stiffness is part of T_a^* , which is a quasi-steady aerodynamic load.

6 / 152 / The matrix " P_u " should not be premultiplied by M^{-1} .
>>> You are correct.

6 / 154 / Why is Y_{qdd} included? As indicated next, qdd can be derived from q_d , q , p , and u , so, including Y_{qdd} is redundant; the acceleration-related terms can be captured directly within Y_{q_d} , Y_q , Y_p , and Y_u .
>>> You are correct, Y_{qdd} is introduced for convenience. If an accelerometer is present in the structure, and this measured acceleration is easily expressed in terms of the acceleration of the degrees of freedom, then the user can input this simple acceleration relationship into the matrix Y_{qdd} . Alternatively, the user can express the measured acceleration in terms of q_d , q , p and u directly, in which case Y_{qdd} is not used. If an automated linearization procedure is used to determine the Y_* matrices, then Y_{qdd} should be skipped since it would be redundant. We now attempt to explain this in the text, using tilde notations for the output equation with acceleration.

9 / 212 / Figure 2b is a bit hard to understand and could be clarified a bit more in the text.
>>> Thank you for your comment. The figure was indeed hard to understand, and it was chosen to remove it altogether, since it was leading to a long discussion in the following paragraph. The main point was that the estimated wind speed can be different from the spatial average wind speed over the rotor, and this difference is not necessarily an "error". The estimated wind speed is, by the current definition, the best wind speed such that the tabulated aerodynamic torque matches the current unsteady aerodynamic torque. Another point was that region 0 needs a dedicated wind speed estimation, something which was already captured by the right figure. These are issues/remarks related to wind speed estimation and are digression for the topic of this article, so we chose to keep these discussions to

a minimum. We now only briefly mention these points. Hopefully, avoiding these discussions will clarify the paper and make it shorter.

11 / 258 / Is there a reason the inertia of the RNA is not accounted for in the model, i.e. a $M_{RNA} \cdot \ddot{t}$ term?

>>> The RNA inertia is part of the mass matrix term M given in equation 1. The following precision was added in section 3.3: "Velocity transformation matrices are used to convert individual component matrices (e.g. blades, nacelle) into the global system matrices. The mass matrix thereby comprise the inertia terms from the tower and RNA."

Technical Corrections (Page / Line / Comment):

2 / 21 / Change "extended" to "extend-ing"

2 / 39 / Change "approach" to "approaches"

2 / 43 / Add a period at the end of the sentence.

5 / 119 / Change " X_y " to " X_u ".

5 / 122 / Presumably " t " represents a transpose? Please clarify.

7 / 160 / Change " X_{x_d} " to " $X_{x,d}$ ".

14 / 310 / Change "quantifies" to "quantified".

>>> Thank you for noticing these errors, they have been corrected now.

12 / 288 / Do you mean Q and R matrices, as used in section 2.3?

>>> You are correct, this was erroneous.

Augmented Kalman filter with a reduced mechanical model to estimate tower loads on an ~~onshore~~ land-based wind turbine: a ~~digital twin~~ digital-twin concept

Emmanuel Branlard¹, Dylan Giardina¹, and Cameron S. D. Brown²

¹National Renewable Energy Laboratory, Golden, CO 80401, USA

²Ørsted, Nesa Allé 1, 2820 Gentofte, Denmark

Correspondence: E. Branlard (emmanuel.branlard@nrel.gov)

Abstract. ~~The paper~~ This article presents an application of the Kalman filtering technique to estimate loads on a wind turbine. The approach combines a mechanical model and a set of measurements to estimate signals that are not available in the measurements, such as ~~the~~ wind speed, thrust, tower position, and tower loads. The model is ~~several fold faster than real-time~~ severalfold faster than real time and is intended to be run online, for instance, to evaluate real-time fatigue life consumption of a field turbine using a digital twin, ~~perform condition monitoring, or assess loads for dedicated control strategies~~. The mechanical model is built using a ~~Rayleigh-Ritz~~ Rayleigh–Ritz approach and a set of joint coordinates. ~~The paper presents~~ We present a general method and ~~illustrates~~ illustrate it using a ~~2-degrees-of-freedom~~ 2-degrees-of-freedom model of a wind turbine ~~and~~ and using rotor speed, generator torque, pitch, and tower-top acceleration as measurement signals. The different components of the model are tested individually. The overall method is evaluated by computing the errors in estimated tower bottom equivalent moment from a set of simulations. From this preliminary study, it appears that the tower bottom equivalent moment is obtained with about 10% accuracy. The limitation of the model and the required steps ~~forwards~~ forward are discussed.

1 Introduction

Wind turbines are designed and optimized for a given site ~~using numerical tools, and, a statistical assessments or class definition using both numerical tools and a statistical assessment~~ of the environmental conditions the turbine will experience. The uncertainty on the tools and data are accounted for using multiplicative safety factors ~~which that~~ are determined from a combination of experience and specifications by the standards. Overconservative safety factors will imply unnecessary costs ~~which may be later on alleviated by extended the life time that may be alleviated later on by extending the lifetime~~ of a project. An ~~under-estimate~~ underestimate of the safety factor will likely lead to catastrophic failures. Once a design is complete and the product is in place, is it possible to predict what the ~~life-time~~ lifetime of the wind turbine will be?

Digital twins are becoming increasingly popular to follow the life cycle of a physical system. This concept is used to bridge the gap between the ~~modelling~~ modeling and measurement realm: ~~real-time-measurement~~ real-time measurements from the physical system are communicated to a digital system, and this information is combined with a numerical model to estimate the state of the system and potentially predict its evolution. A Kalman filter (KF) ~~is an example of~~ is one example of a

technique that can be used: it combines a model of a system with a set of measurements on ~~this~~-that system to predict additional variables, such as positions or loads at points where no measurements are available. ~~Other approaches are for instance: inverse methods, or neural network methods~~In this study, we focus on Kalman filter methods, but other load estimation techniques may be used, such as lookup tables (Mendez Reyes et al., 2019), modal expansion (Iliopoulos et al., 2016), machine learning (Evans et al., 2018), neural networks (Schröder et al., 2018), polynomial chaos expansion (Dimitrov et al., 2018), deconvolution (Jacquelin et al., 2003), or load extrapolation (Ziegler et al., 2017).

Kalman filters have been extensively used in control engineering with a wide range of applications. Auger et al. (2013) provide a review of some industrial applications. Load estimation using Kalman filtering are found, for example, in the following references: Ma and Ho (2004) and Eftekhari Azam et al. (2015). In the context of wind energy, wind speed estimation is critical for the determination of the dynamics of the system. This topic was ~~for instance~~-investigated using parametric models by ~~Bozkurt et al. (2014)~~, Bozkurt et al. (2014); using Kalman filters by Østergaard et al. (2007), Knudsen et al. (2011), ~~or Song et al. (2017)~~, and using Luenberger-type observer by and Song et al. (2017); and using Luenberger-type observer by Hafidi and Chauvin (2012). A comparison of wind speed estimation technique is found in ~~Soltani et al. (2013)~~, Soltani et al. (2013). The techniques were extended to also estimate the wind shear and turbine misalignments(~~see.g.~~; see, for example, Bottasso et al. (2010), Simley and Pao (2016), ~~Bertelè et al. (2018)~~), and Bertelè et al. (2018). Kalman filtering has been used to estimate rotor loads and wind speed in application to rotor controls by Boukhezzar and Siguerdidjane (2011).

Kalman filtering was recently used by Belloli (2019) to estimate the sea state based on the knowledge of the offshore platform position. ~~More general~~-General approaches use Kalman filtering in combination with a model of the full wind turbine dynamics. These ~~approach~~-approaches were used for wind speed estimation and load alleviation via individual pitch control (~~Selvam et al. (2009)~~, Bottasso and Croce (2009)), Selvam et al. 2009; Bottasso and Croce 2009) and for online estimation of mechanical loads ~~Bossanyi (2003)~~(Bossanyi, 2003). An example of estimating tower loads with the acceleration sensor is ~~for instance found in the report of Hau (2008)~~. Bossanyi et al. found in Hau (2008). Bossanyi et al. (2012) compared the observed rotor and tower loads with measurements , and investigated the potential of the control method to reduce damage equivalent loads (~~Bossanyi et al., 2012~~).

The methodology presented in this article uses an augmented ~~KF (Lourens et al. (2012))~~ Kalman filter (Lourens et al., 2012) to estimate loads on the wind turbine based on measurement signals commonly available in the nacelle. The method builds on the approach used by ~~Bossanyi et al. and Lourens et al~~Bossanyi et al. (2012) and Lourens et al. (2012). The method of ~~Lourens et al.~~Lourens et al. (2012) is generalized. On the other hand, the expression of the mechanical system may be seen as simplified compared to the approach of ~~Bossanyi et al.: a Rayleigh-Ritz~~Bossanyi et al. (2012): a Rayleigh-Ritz formulation is used and the system is not further linearized. The equations are given in full for a ~~2-degrees-of-freedom~~2-degrees-of-freedom (DOF) system, and the source code is made available online. The time series of estimated loads are applied to assess the fatigue life consumption of the turbine components using the rainflow counting method. The study focuses on the determination of tower loads of ~~onshore wind turbine~~. land-based wind turbines. A scheme of the method is provided in Figure 1. The numerical model of the wind turbine relies on a ~~Rayleigh-Ritz~~Rayleigh-Ritz shape-function approach with reduced numbers of ~~degrees of freedom (Branlard (2019a))~~DOF (Branlard, 2019a). The wind speed is estimated using an approach similar to Østergaard

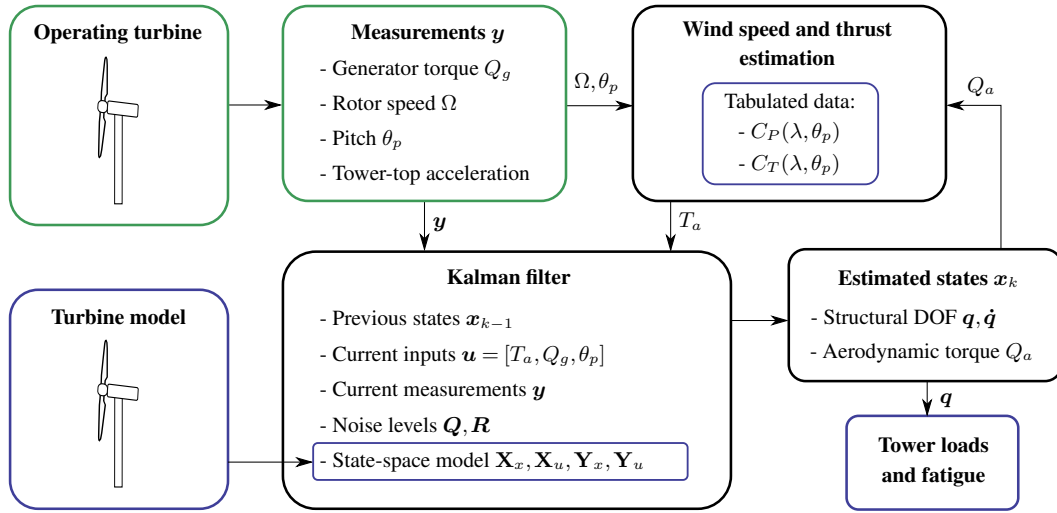


Figure 1. Main components of the model: wind turbine measurements and a turbine model are combined to estimate tower loads. A wind speed estimator and a Kalman filter algorithm are used in the estimation. Turbine model dependencies are framed in blue.

et al. (2007), and the thrust force estimation is based on this wind speed estimate. The generator torque, the rotor speed, and the tower-top accelerations are used as measurements and combined with the numerical model with an augmented KF within an augmented Kalman filter. The time series of loads in the tower are determined based on the tower shape function and the tower degrees of freedom, and the fatigue loads are computed from this signal. It is noted that the method is expected to be more accurate at the tower bottom than the tower top because rotor asymmetric loading cannot be captured from the single acceleration measurement.

The first part Section 2 presents the different components required for this work: the augmented KF Kalman filter, the numerical model of the turbine, and the estimators for the wind speed, thrust, tower load, and fatigue. Simple illustrations and validation results for the different components of the model are provided in a second part. The third part Section 3. Section 4 presents full applications, but limited to simulations. Discussions and conclusions follow.

2 Description of the models

2.1 Example for a 2DOF-2 DOF wind turbine model

We start this section by with an illustrative example before describing the different parts of the model in their general form. A wind turbine is here modelled modeled here using 2 DOF: (1) the generalized coordinate associated with the fore-aft (FA) bending of the tower, q_t , and (2) the shaft rotation, ψ . The tower bending is associated with a shape function, $\Phi_t(z)$, such that the FA fore-aft displacement of a point at height z and at time t is given by $u(z, t) = q_t(t)\Phi_t(z)$. The shape function is normalized to unity at the tower-top tower top, and q_t is then equal to the FA fore-aft displacement at the tower-top tower top

(see Figure 2). The equations of motion of the system are:

$$\begin{bmatrix} M & 0 \\ 0 & J \end{bmatrix} \begin{bmatrix} \ddot{q}_t \\ \ddot{\psi} \end{bmatrix} + \begin{bmatrix} C & 0 \\ 0 & 0 \end{bmatrix} \begin{bmatrix} \dot{q}_t \\ \dot{\psi} \end{bmatrix} + \begin{bmatrix} K & 0 \\ 0 & 0 \end{bmatrix} \begin{bmatrix} q_t \\ \psi \end{bmatrix} = \begin{bmatrix} T_a^* \\ Q_a - Q_g \end{bmatrix} \quad (1)$$

where M , C , and K are the generalized mass, damping, and stiffness, respectively, associated with the fore-aft DOF; J is the drivetrain inertia; T_a^* and Q_a are the aerodynamic thrust and torque, respectively; and Q_g is the generator torque. A star is used as upper-script of superscript asterisk is used on the thrust to indicate that using the thrust directly is a rough approximation. A more elaborate expression of the generalized force acting on q_t is given in Section 3.3. The determination of M , C , and K is discussed in Branlard (2019a). For the NREL-5MW National Renewable Energy Laboratory (NREL) 5 MW turbine, the values are: $M = 4.4e^5$ kg, $D = 2.5e^4$ kg s⁻¹, $K = 2.7e^6$ kg s⁻², and $J = 4.3e^7$ kg m². We tuned the damping term C to account for aerodynamic damping, as mentioned in Section 3.3. Aerodynamic stiffness is included in T_a^* . In this example, the system of equations is only-coupled-coupled only via the aerodynamic loads.

The following measurements are usually readily available on any commercial wind turbine: the generator power, P_g ; the blade pitch angle, θ_p ; the rotor rotational speed, $\Omega \triangleq \dot{\psi}$; and the tower-top acceleration in the fore-aft direction, \ddot{q}_t . The knowledge of the generator power, speed, and losses allows to estimate the generator torque for the estimation of the generator torque, Q_g . In this study, the generator torque is assumed to be known. We will use an augmented KF-Kalman filter concept to combine these measurements with the mechanical model to estimate the state of the system. The KF-Kalman filter algorithm requires linear state and output equations. The state vector is assumed to be $\mathbf{x} = [q_t, \psi, \dot{q}_t, \dot{\psi}, Q_a]$. The fact that some of the loads were included into the state vector is referred to as “state augmentation.” The choice of loads to include in the state vector is not unique and will lead to different state equations. Using this choice for \mathbf{x} , we write Equation 1 is-written into the following state equation:

$$\begin{bmatrix} \dot{q}_t \\ \dot{\psi} \\ \ddot{q}_t \\ \ddot{\psi} \\ \dot{Q}_a \end{bmatrix} = \begin{bmatrix} 0 & 0 & 1 & 0 & 0 \\ 0 & 0 & 0 & 1 & 0 \\ -M^{-1}K & 0 & -M^{-1}C & 0 & 0 \\ 0 & 0 & 0 & 0 & J^{-1} \\ 0 & 0 & 0 & 0 & 0 \end{bmatrix} \begin{bmatrix} q_t \\ \psi \\ \dot{q}_t \\ \dot{\psi} \\ Q_a \end{bmatrix} + \begin{bmatrix} 0 & 0 & 0 \\ 0 & 0 & 0 \\ M^{-1} & 0 & 0 \\ 0 & -J^{-1} & 0 \\ 0 & 0 & 0 \end{bmatrix} \begin{bmatrix} T_a^*(\dot{\psi}, Q_a, \theta_p) \\ Q_g \\ \theta_p \end{bmatrix} \quad (2)$$

wherefor-simplicity-, for simplicity, the time derivatives of the aerodynamic torque is assumed to be zero, an assumption referred to as “random walk force model.” This assumption accounts of-for saying that the estimate of the torque at the next time step is likely to be close to the one at the current time step. Improvements on this will be discussed in Section 5. The thrust is determined based on the rotor speed, the aerodynamic torque, and the pitch angle, pitch angle using tabulated data, as described in Section 2.4. The output equation relates the measurements to the states and inputs as follows:

$$\begin{bmatrix} \ddot{q}_t \\ \dot{\psi} \\ Q_g \\ \theta_p \end{bmatrix} = \begin{bmatrix} -M^{-1}K & 0 & -M^{-1}C & 0 & 0 \\ 0 & 0 & 0 & 1 & 0 \\ 0 & 0 & 0 & 0 & 0 \\ 0 & 0 & 0 & 0 & 0 \end{bmatrix} \mathbf{x} + \begin{bmatrix} M^{-1} & 0 & 0 \\ 0 & 0 & 0 \\ 0 & 1 & 0 \\ 0 & 0 & 1 \end{bmatrix} \begin{bmatrix} T_a^* \\ Q_g \\ \theta_p \end{bmatrix} \quad (3)$$

Equation 2 and Equation 3 are used within a ~~KF~~-Kalman filter algorithm to estimate the ~~states~~-state's vector based on the measurements. The estimated time series of q_t , together with its associated shape function Φ_t , are used to determine the bending moments within the tower and estimate tower fatigue loads, based on the method presented in Section 2.5. Results from this simple model will be provided in Section 3. The ~~remaining paragraphs~~-rest of this section ~~generalize~~-generalizes the approach presented.

2.2 Mechanical model of the wind turbine

The wind turbine is described using a set of ~~degrees-of-freedom (DOF)~~-DOF that consist of ~~joints~~-joint coordinates and shape ~~functions~~-function coordinates. The method was described in previous work (Branlard, 2019a), and the source code made available online ~~via~~ via a library called YAMS (Branlard, 2019b). Similar approaches are ~~for instance~~-used in the elastic codes Flex and OpenFAST (OpenFAST, 2020). The advantage of the method is that the system can be described with few DOF. The number of DOF is between 2 and 30~~DOF~~, whereas traditional finite element methods require in the order of ~~one-thousand~~ 1000 DOF.

The only joint coordinate retained in the current model is the shaft azimuthal position, noted ψ . The shaft torsion ~~and~~ nacelle yaw and tilt joints can be added without difficulty. The tower and blades are represented using a set of shape functions taken as the first mode shapes of these components. The shape functions of the tower are assumed to be the same in the ~~FA and side-side (SS)~~-fore-aft and side-side directions, which are respectively aligned with the x and y directions (see Figure 2). The number of shape functions are noted n_{xt} , n_{yt} , and n_b for the tower ~~FA, tower SS~~-fore-aft, tower side-side, and blade ~~respectively. Writing, respectively. Using~~ B as the number of blades ~~and~~ n_s as the number of DOF representing the shaft, the total number of DOF is: $n_q = n_s + Bn_b + n_{xt} + n_{yt}$. The tower DOF are written as $q_{xt,i}$, with $i \in [1..n_{xt}]$ and $q_{yt,i}$ with $i \in [1..n_{yt}]$. Similar notations are used for the blade DOF.

The equation of motions are established using Lagrange's equation. The example presented in Section 2.1 corresponds to $n_s = 1$, $n_b = 0$, $n_{t,SS} = 0$, and $n_{t,FA} = 1$. An example for a ~~5DOF system~~, 5 DOF system with $n_s = 1$, $B = 2$, $n_b = 1$, $n_{t,SS} = 0$, and $n_{t,FA} = 1$ ~~is~~ is given in Branlard (2019a). In the general case, the ~~equation of motions~~-equations of motion are described as:

$$M\ddot{\mathbf{q}} + C\dot{\mathbf{q}} + K\mathbf{q} = \mathbf{f} \quad \rightarrow \quad \begin{bmatrix} \dot{\mathbf{q}} \\ \ddot{\mathbf{q}} \end{bmatrix} = \begin{bmatrix} \mathbf{0} & \mathbf{I} \\ -M^{-1}K & -M^{-1}C \end{bmatrix} \begin{bmatrix} \mathbf{q} \\ \dot{\mathbf{q}} \end{bmatrix} + \begin{bmatrix} \mathbf{0} \\ M^{-1}\mathbf{f} \end{bmatrix} \quad (4)$$

where M , C , and K are the mass, damping, and stiffness matrices, ~~respectively~~; \mathbf{q} is the vector of DOF; and \mathbf{f} is the vector of generalized loads acting on the DOF. An inconvenience of the method is that the mass matrix is a ~~non-linear~~-nonlinear function of the DOF. The main assumption of this work is that the ~~non-linearities~~-nonlinearities can be discarded as a first approximation. This assumption is further discussed in Section 5.

2.3 Augmented Kalman filter applied to a mechanical system

~~A description~~-Descriptions of the standard ~~KF~~-Kalman filter can be found ~~e.g. in the textbook of~~ in Grewal and Andrews (2014) or Zarchan and Musoff (2015). The algorithm will not be detailed in this ~~paper~~-article. The method ~~expect a~~-expects state and

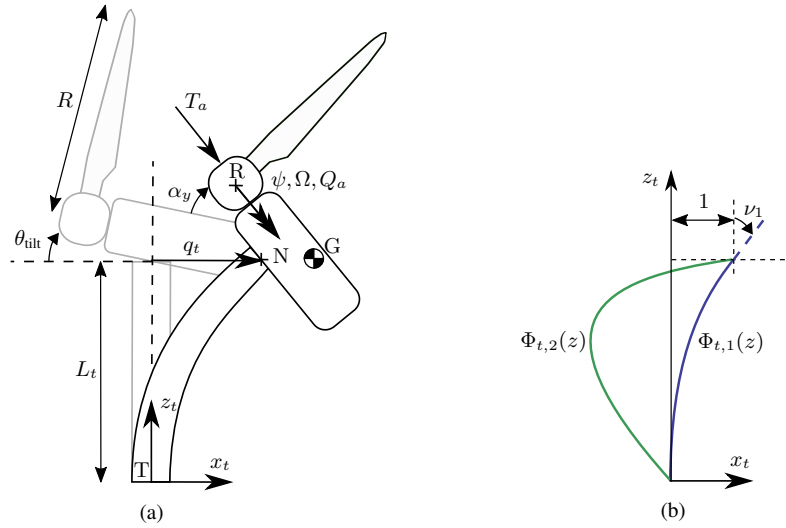


Figure 2. (a) Notations for the wind turbine model and (b) example of shape functions used for the tower. Definition of points: T: tower bottom; N: tower top; G: center of mass of the rotor nacelle assembly; R: rotor center. The shape functions are normalized to unity at point N. The slope at the extremity of the first shape function is written $\nu_1 \triangleq \frac{d\Phi_{t,1}}{dz}(L_t)$.

output equations of the following form:

$$\dot{\mathbf{x}} = \mathbf{X}_x \mathbf{x} + \mathbf{X}_u \mathbf{u} + \mathbf{w}_x \quad (\text{state equation}) \quad (5)$$

$$\mathbf{y} = \mathbf{Y}_x \mathbf{x} + \mathbf{Y}_u \mathbf{u} + \mathbf{w}_y \quad (\text{output/measurement equation}) \quad (6)$$

where \mathbf{x} , \mathbf{u} , and \mathbf{y} are the state, input, and measurement vectors, respectively; \mathbf{X}_x , \mathbf{X}_y , \mathbf{X}_u , \mathbf{Y}_x , and \mathbf{Y}_u are Jacobian matrices describing the expected relationships between measurements, states, and inputs; and \mathbf{w}_x and \mathbf{w}_y are Gaussian uncorrelated noises associated with the state-space model and measurements, respectively, of which the associated covariance matrices are noted $\mathbf{Q} = E[\mathbf{w}_x \mathbf{w}_x^t]$ and $\mathbf{R} = E[\mathbf{w}_y \mathbf{w}_y^t]$, with $E[\mathbf{w}_x \mathbf{w}_y^t] = \mathbf{0}$ and, E the expected value operator, and the subscript t represents a transpose. We will develop these equations in the case of a mechanical system that follows the general form of Equation 4. Specific applications will be given in Section 3 and Section 4.

Different approaches can be used to write Equation 4 in the form of Equation 5, depending how the force vector is to be treated. In a first approach, the forces can be considered to be inputs $\mathbf{f} = \mathbf{u}$, in which case Equation 4 is directly in the form of Equation 5, with $\mathbf{x} = [\mathbf{q}, \dot{\mathbf{q}}]$. This implies that we have full knowledge of the forces acting on the system at every time step, which is unlikely. In a second approach, the forces can be assumed to be part of the system noise, \mathbf{w}_x , which would lead to $\mathbf{x} = [\mathbf{q}, \dot{\mathbf{q}}]$ and $\mathbf{B} = \mathbf{0}$. This is obviously a crude approximation since because the forces acting on the system are non-stochastic, and, nonstochastic, and we likely have some knowledge on of them. In the intermediate approach introduced by Lourens et al. (Lourens et al., 2012) Lourens et al. (2012), some of the forces are included in the system noise, and others as part of the states. The We write the reduced set of loads that are part of the states is written state \mathbf{p} , of length n_p , and the

150 full force vector is assumed to be approximated by: $\mathbf{f} \approx \mathbf{S}_p \mathbf{p}$, where \mathbf{S}_p is a matrix of dimension $n_q \times n_p$. The reduced set of forces, \mathbf{p} , is integrated into the state vector as: $\mathbf{x} = [\mathbf{q}, \dot{\mathbf{q}}, \mathbf{p}]$. This process is referred to as “state augmentation.”

We introduce a generalized approach and assume that the forces are a combination of states, inputs, and unknown noise:

$$\mathbf{f} \approx \mathbf{F}_q \mathbf{q} + \mathbf{F}_{\dot{q}} \dot{\mathbf{q}} + \mathbf{F}_p \mathbf{p} + \mathbf{F}_u \mathbf{u} + \mathbf{w}_f \approx \mathbf{F}_q \mathbf{q} + \mathbf{F}_{\dot{q}} \dot{\mathbf{q}} + \mathbf{F}_p \mathbf{p} + \mathbf{F}_u \mathbf{u} \quad (7)$$

where the \mathbf{F}_\bullet matrix represent the Jacobian of the force vector with respect to vector \bullet , and \mathbf{w}_f are unknown forces that are
 155 assumed to be part of system disturbance, \mathbf{w}_x . The terms \mathbf{F}_q and $\mathbf{F}_{\dot{q}}$ are linearized stiffness and damping terms. These terms are zero if their contributions are already included in the definitions of \mathbf{K} and \mathbf{C} . In practice, the linearization of the force vector may not be possible, and assumed relationships or engineering models are used. As an example, if \mathbf{p} ~~contain~~ contains the thrust force and \mathbf{f} the moment at the tower base, the appropriate element of \mathbf{F}_p could be set with the lever arm between ~~tower-top~~ the tower top and tower base.

160 This approach allows us to use the knowledge we have of some of the main loads acting on the system and express their dynamics into the state-space equation. The forces may ~~for instance~~, for instance, be assumed to follow a ~~first-order~~ first-order system as follows:

$$\dot{\mathbf{p}} = \mathbf{P}_q \mathbf{q} + \mathbf{P}_{\dot{q}} \dot{\mathbf{q}} + \mathbf{P}_p \mathbf{p} + \mathbf{P}_u \mathbf{u} \quad (8)$$

where the \mathbf{P}_\bullet matrices are obtained from a knowledge of the force evolution. ~~Second-order~~ A second-order system could also
 165 be introduced, in which case the state needs to be augmented with both \mathbf{p} and $\dot{\mathbf{p}}$ (“random walk” force model). For simplicity, the applications used in this work will assume $\dot{\mathbf{p}} = \mathbf{0}$, but future work will investigate the benefit of using ~~first-order~~ first-order systems for the evolution of the forces.

Inserting Equation 7 into Equation 4, introducing $\mathbf{x} = [\mathbf{q}, \dot{\mathbf{q}}, \mathbf{p}]$, and using Equation 8, we obtain a state equation of the form of Equation 5 is obtained:

$$170 \quad \mathbf{X}_x = \begin{bmatrix} \mathbf{0} & \mathbf{I} & \mathbf{0} \\ -\mathbf{M}^{-1}(\mathbf{K} - \mathbf{F}_q) & -\mathbf{M}^{-1}(\mathbf{C} - \mathbf{F}_{\dot{q}}) & \mathbf{M}^{-1}\mathbf{F}_p \\ \mathbf{P}_{\dot{q}} & \mathbf{P}_q & \mathbf{P}_p \end{bmatrix}, \quad \mathbf{X}_u = \begin{bmatrix} \mathbf{0} \\ \mathbf{M}^{-1}\mathbf{F}_u \\ \mathbf{P}_u \end{bmatrix} \quad (9)$$

The measurements are assumed to be a combination of the acceleration, velocity, displacements, loads, and inputs:

$$\mathbf{y} \approx \tilde{\mathbf{Y}}_{\ddot{q}} \ddot{\mathbf{q}} + \tilde{\mathbf{Y}}_{\dot{q}} \dot{\mathbf{q}} + \tilde{\mathbf{Y}}_q \mathbf{q} + \tilde{\mathbf{Y}}_p \mathbf{p} + \tilde{\mathbf{Y}}_u \mathbf{u} \quad (10)$$

~~Inserting the acceleration~~ The matrix $\tilde{\mathbf{Y}}_{\ddot{q}}$ is here introduced for convenience when a simple relationship exists between outputs and DOF accelerations, but this term can be omitted altogether and should not be double-counted. Indeed, the acceleration, $\ddot{\mathbf{q}}$,
 175 can be isolated from Equation 4 ~~into, an output~~, and then expressed as a function of $\dot{\mathbf{q}}$, \mathbf{p} , and \mathbf{u} . If an automated linearization procedure is used, then the acceleration term should be skipped because it would otherwise be redundant. The output relationship would then be:

$$\mathbf{y} \approx \mathbf{Y}_{\dot{q}} \dot{\mathbf{q}} + \mathbf{Y}_q \mathbf{q} + \mathbf{Y}_p \mathbf{p} + \mathbf{Y}_u \mathbf{u} \quad (11)$$

The link between the two formulations is provided using Equation 4, giving:

$$180 \quad \mathbf{Y}_q = \tilde{\mathbf{Y}}_q - \tilde{\mathbf{Y}}_{\dot{q}} \mathbf{M}^{-1} \mathbf{K}, \quad \mathbf{Y}_{\dot{q}} = \tilde{\mathbf{Y}}_{\dot{q}} - \tilde{\mathbf{Y}}_{\ddot{q}} \mathbf{M}^{-1} \mathbf{C}, \quad \mathbf{Y}_p = \tilde{\mathbf{Y}}_p + \tilde{\mathbf{Y}}_{\dot{q}} \mathbf{M}^{-1} \mathbf{F}_p, \quad \mathbf{Y}_u = \tilde{\mathbf{Y}}_u + \tilde{\mathbf{Y}}_{\dot{q}} \mathbf{M}^{-1} \mathbf{F}_u \quad (12)$$

An output equation of the form of Equation 6 is ~~obtained, with:~~ directly obtained as:

$$\mathbf{Y}_x = \begin{bmatrix} \mathbf{Y}_q & \mathbf{Y}_{\dot{q}} & \mathbf{Y}_p \end{bmatrix}, \quad \mathbf{Y}_u = \underline{\underline{u}} + \underline{\underline{\mathbf{Y}}_{\dot{q}}}^{-1} \underline{\underline{u}} \quad (13)$$

Equation 9 and Equation 13 form the bridge between the definition of the mechanical model and the state and output equations needed by the ~~KF~~ Kalman filter algorithm.

185 Equation 5 and Equation 6 are in continuous form, whereas the ~~KF~~ Kalman filter algorithm uses discrete forms. The discrete ~~form-forms~~ of the matrices perform the time integration of the states from one time step to the next, namely: ~~$\mathbf{x}_{k+1} = \mathbf{X}_{x,d} \mathbf{x}_k + \mathbf{X}_{u,d} \mathbf{u}_k$~~ $\mathbf{x}_{k+1} = \mathbf{X}_{x,d} \mathbf{x}_k + \mathbf{X}_{u,d} \mathbf{u}_k$, where the subscript d indicates the discrete form of the matrices and k is the ~~time-step~~ time-step index. The matrix $\mathbf{X}_{x,d}$ is referred to as the “fundamental matrix.” For time-invariant systems, this matrix may be obtained using Laplace ~~transform-transform~~ or by Taylor-series expansion (Zarchan and Musoff, 2015). For a
190 given time step, Δt , the discrete matrices corresponding to \mathbf{X}_x and \mathbf{X}_u are:

$$\begin{aligned} \mathbf{X}_{x,d} &= e^{\mathbf{X}_x \Delta t} = \mathbf{I} + \mathbf{X}_x \Delta t + \frac{(\mathbf{X}_x \Delta t)^2}{2!} + \dots \approx \mathbf{I} + \mathbf{X}_x \Delta t \\ \mathbf{X}_{u,d} &= \int_0^{\Delta t} \mathbf{X}_{x,d}(\tau) \mathbf{X}_u d\tau \approx [\mathbf{X}_{x,d} - \mathbf{I}] \mathbf{X}_x^{-1} \mathbf{X}_u \approx \mathbf{X}_u \Delta t \end{aligned} \quad (14)$$

The approximation in Equation 14 is effectively a ~~first-order~~ first-order forward Euler time integration. The ~~matrix-matrices~~ \mathbf{Y}_x and \mathbf{Y}_u remain unchanged by the discretization ~~since the ouput~~ because the output equation is an algebraic equation involving
195 quantities at the same time step.

Many choices are possible as to how the model may be formulated~~-,~~ including which forces should be accounted for in the reduced set, \mathbf{p} , which forces should be assumed to be obtained from the inputs, which models to use for the \mathbf{P} matrices, ~~etc.~~ Since the and so on. This study is limited to ~~onshore-land-based~~ wind turbines, and therefore the main loads are the aerodynamic thrust and torque. A subtlety to account for ~~;~~ is that some of the forces of the model presented in Equation 4 are
200 generalized forces, ~~which are projection and are projections~~ of loads onto the shape functions (Branlard, 2019a). An example will be given in Section 3.3.

~~The~~ When possible, the Jacobian matrices introduced should be determined by linearization about an operating point. The mass matrix should also be linearized about such ~~point-a point~~ point. In the current work, the ~~non-linearities~~ nonlinearities are either neglected ~~;~~ or directly inserted into the expression presented without performing a linearization. This crude simplification will
205 be discussed in Section 5, in light of the results presented in Section 3 and Section 4.

2.4 Wind speed and thrust estimation

~~In this paragraph~~ In this section, Q_a , θ_p , and Ω are assumed to be given. The aerodynamic power and thrust coefficients, C_P and C_T , are also assumed to be known as a function of the pitch angle and ~~tip-speed~~ tip-speed ratio, $\lambda = \Omega R / U_0$, where R is

the rotor radius and U_0 is the wind speed. The functions $C_P(\lambda, \theta_p)$ and $C_T(\lambda, \theta_p)$ are estimated by running a parametric set of simulations at constant operating conditions. ~~Some uncertainty is here present~~ There is some uncertainty here as to whether the real turbine ~~does~~ performs as predicted by these functions. This question will be considered in Section 5. The aerodynamic torque is computed from the tabulated data as:

$$Q_{a,\text{tab}}(U_0, \Omega, \theta_p) = \frac{1}{2} \rho \pi R^2 \frac{U_0^3}{\Omega} C_P \left(\frac{\Omega R}{U_0}, \theta_p \right) \quad (15)$$

~~The wind speed is obtained by solving the following non-linear constraint equation for u_{est} :~~

215 Find u_{est} , such that $Q_a - Q_{a,\text{tab}}(u_{\text{est}}, \Omega, \theta_p) = 0$

where ρ is the air density, which is another potential source of uncertainty to be considered when dealing with measurements. The wind speed is obtained by solving the following nonlinear constraint equation for u_{est} :

$$\text{Find } u_{\text{est}}, \text{ such that } Q_a - Q_{a,\text{tab}}(u_{\text{est}}, \Omega, \theta_p) = 0 \quad (16)$$

The wind speed determined by this method is assumed to be the effective wind speed acting over the rotor area. A correction for nacelle displacements is discussed in Section 5. The aerodynamic thrust is estimated from this wind speed as:

$$T_{a,\text{est}} = T_{a,\text{tab}}(u_{\text{est}}, \Omega, \theta_p), \quad \text{with} \quad T_{a,\text{tab}}(U_0, \Omega, \theta_p) = \frac{1}{2} \rho \pi R^2 U_0^2 C_T \left(\frac{\Omega R}{U_0}, \theta_p \right) \quad (17)$$

2.5 Tower loads and fatigue estimation

The deflection of the tower, U , in the x or y directions ~~;~~ at a given height, z , and a given time, t , is given by the sum of the tower shape functions scaled by the tower degrees of freedom:

225
$$U_x(z, t) = \sum_i q_{xt,i}(t) \Phi_{t,i}(z), \quad U_y(z, t) = \sum_i q_{yt,i}(t) \Phi_{t,i}(z) \quad (18)$$

The curvature, κ , is obtained by differentiating the deflection twice, giving:

$$\kappa_x(z, t) = \sum_i q_{xt,i}(t) \frac{d^2 \Phi_{t,i}}{dz^2}(z), \quad \kappa_y(z, t) = \sum_i q_{yt,i}(t) \frac{d^2 \Phi_{t,i}}{dz^2}(z) \quad (19)$$

The bending moments along the tower ~~heights~~ height are then obtained from the curvatures using Euler beam theory:

$$M_y(z, t) = EI(z) \kappa_x(z, t), \quad M_x(z, t) = EI(z) \kappa_y(z, t) \quad (20)$$

230 where EI is the bending stiffness of a given tower cross section. The time series of bending moment are processed using a ~~rain-flow~~ rainflow counting algorithm to estimate the equivalent loads and damage (International Standard IEC, Workgroup 3, 2005).

3 Simple applications and validations

3.1 Wind speed estimation

235 ~~The~~In this section, we illustrate and evaluate the wind speed estimation methodology presented in Section 2.4~~is illustrated and evaluated in this section. Tabulated~~. We computed tabulated C_P and C_T ~~values were obtained for the NREL-5MW for the NREL 5 MW turbine (Jonkman et al., 2009) using the multi-physics simulation tool OpenFAST (OpenFAST, 2020). A turbulent simulation was devised such as~~We devised a turbulent simulation to sweep through the main operating regions of the wind turbine within a ~~10-10~~ min period, namely: the startup region (~~region~~Region 0), the optimal C_p tracking region (~~region~~Region 1), rotor-speed regulation (~~region~~Region 2), and power regulation (~~region~~Region 3). ~~For the NREL-5MW turbine region-Region 2 has a small span and it is here gathered with region for the NREL 5 MW turbine, so it is gathered with Region 3. The turbine was simulated~~We simulated the turbine with all the DOFs turned on ~~.The following variables were extracted and extracted the following variables~~ from the simulation at 50 Hz: \bar{u}_{ref} , the average wind speed at the rotor plane; $Q_{a,\text{ref}}$, the aerodynamic torque; $T_{a,\text{ref}}$, the aerodynamic thrust; Ω_{ref} , the rotational speed; and $\theta_{p,\text{ref}}$, the pitch angle. The wind speed, u_{est} ,
245 was estimated using the method presented in Section 2.4. The results are presented in Figure 3 and ~~commented below~~~~.detailed~~ as follows.

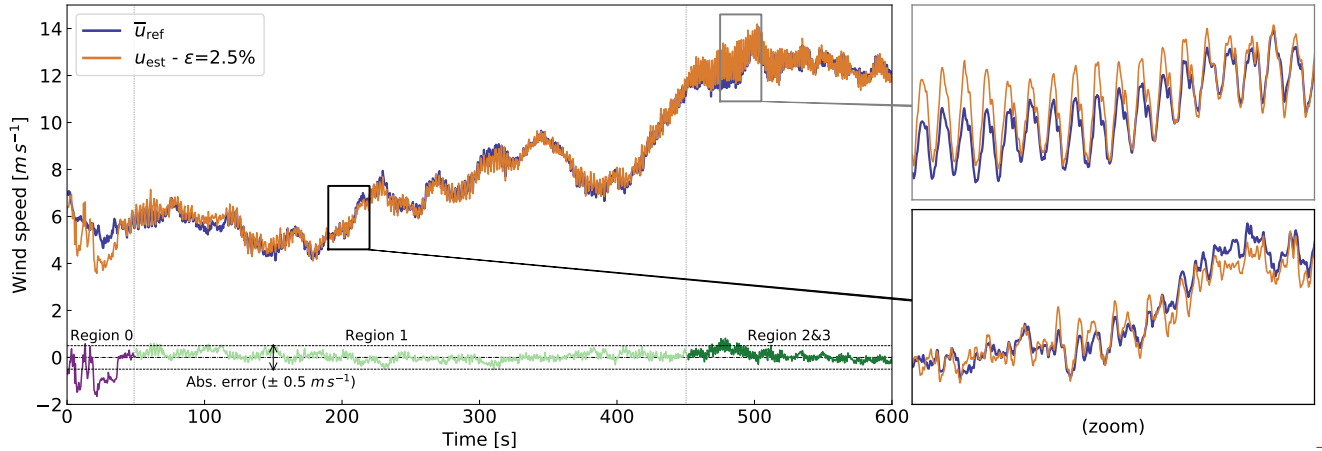


Figure 3. ~~Wind~~Estimated wind speed ~~estimation based on~~ compared to rotor-averaged wind speed for a reference simulation. ~~(Left:)~~Wind speed-time series and absolute error colored by operating regions. Two extracted windows are shown. ~~(Right:)~~Relative error in estimated torque and wind speed colored by operating regions. The probability density function (PDF) is given for each axis.

The absolute error in wind speed is ~~observed to be~~ mostly within ± 0.5 ~~, both values being indicated by two dashed lines on the left figure~~ m s^{-1} . The error is greatest in ~~region~~Region 0, where the generator torque is not yet applied. A separate ~~wind speed-wind-speed~~ method should be devised for this case. The mean relative error for the entire time series is $\epsilon = 2.5\%$. The
250 estimated wind speed is ~~seen~~observed to follow the challenging trends of this time series, matching both the low and high

frequencies. In the top zoom, ~~it is seen that~~ no phase lag is observed in the estimated wind speed, but the estimated value is ~~seen to overshoot.~~

There are several potential sources of errors in the current methodology. One concern is whether the unsteady aerodynamic torque, can be determined using a look-up table that uses instantaneous values. ~~overshooting.~~ The relative error between the unsteady torque $Q_{a,\text{ref}}$ and the tabulated torque, $Q_{a,\text{tab}}(\bar{u}_{\text{ref}}, \Omega_{\text{ref}}, \theta_{p,\text{ref}})$, is used as the x -axis on the right of . A wide range of values is obtained, with the error varying between -40% and 20% . Such estimation of the torque is likely to be accurate only for slow varying wind fields, where the effects of dynamic wake and dynamic stall on the blade loading will be limited. The tabulated method may be improved by accounting for these unsteady aerodynamic effects (discussed in). Another question is whether the effective wind speed, that characterizes the aerodynamic forces on the turbine, is indeed the average wind speed at the rotor plane. The relative error between \bar{u}_{ref} and u_{est} is used as y -axis on the right figure. A large error on this axis may not necessarily indicate Overall, the results from the test case are encouraging. It is not expected that the estimated wind speed is wrong, since indeed this estimated wind speed is such that $Q_a = Q_{a,\text{tab}}(u_{\text{est}}, \Omega_{\text{ref}}, \theta_{p,\text{ref}})$, as a result of the minimization involved in . The estimated wind speed may thus be expected to be different from the rotor averaged ~~corresponds exactly to~~ the rotor-averaged wind speed. During the startup period, the error in wind speed can be large and is uncorrelated to the error in torque, yet a stronger correlation is seen when the turbine is producing power. Looking at the probability density functions given in the right of , it is seen that the errors in torque and wind speed are centered on zero. The fact that both errors are centered on zero, indicate that when the unsteady torque can indeed be obtained using instantaneous values and tabulated data, the (estimated) effective wind speed is close to the average wind speed at the rotor . Other sources of errors are discussed in .

A more thorough study on the questions raised above are left open for future work. Overall, the results from the test case are encouraging. Wind speed ~~Instead, it is a proxy to assess the instantaneous aerodynamic rotor state.~~ Wind-speed estimation is a standard feature of most wind turbine controllers, and it is likely that more advanced features are implemented by manufacturers. Any improvement on the methodology ~~used in the current paper will~~ would be beneficial for the procedure of loads estimation presented in this work.

3.2 Thrust estimation

~~The~~ We compute the estimated thrust, $T_{a,\text{est}}$, using Equation 17 and the wind speed estimated in Section 3.1 ~~is used to estimate the thrust $T_{a,\text{est}}$ with.~~ In Figure 4, we compare the estimated thrust value ~~is compared~~ to the unsteady aerodynamic thrust from the simulation, $T_{a,\text{ref}}$. The values of $T_{a,\text{tab}}(\bar{u}_{\text{ref}}, \Omega_{\text{ref}}, \theta_{p,\text{ref}})$ are also shown in the figure. ~~For this simulation, We observe that the thrust signal was is~~ obtained with a mean relative error of 1.5% over the range of operating conditions considered. ~~Using The use of the estimated wind speed is seen to produce produces~~ thrust values closer to the reference thrust than if \bar{u}_{ref} is used. In line with the discussions of Section 3.1, this ~~could support supports~~ the fact that the estimated wind speed provides an effective velocity , that is consistent with the instantaneous state of the rotor, but different from the ~~rotor-averaged rotor-averaged~~ wind speed. ~~Yet However,~~ it is also possible that compensating errors are at play, or , that the thrust is less sensitive to changes of in wind speed or ~~drive-train drivetrain~~ dynamics than the torque. Despite these open questions, we continue by assuming the ~~method provide that the method provides~~ thrust estimates with sufficient accuracy.

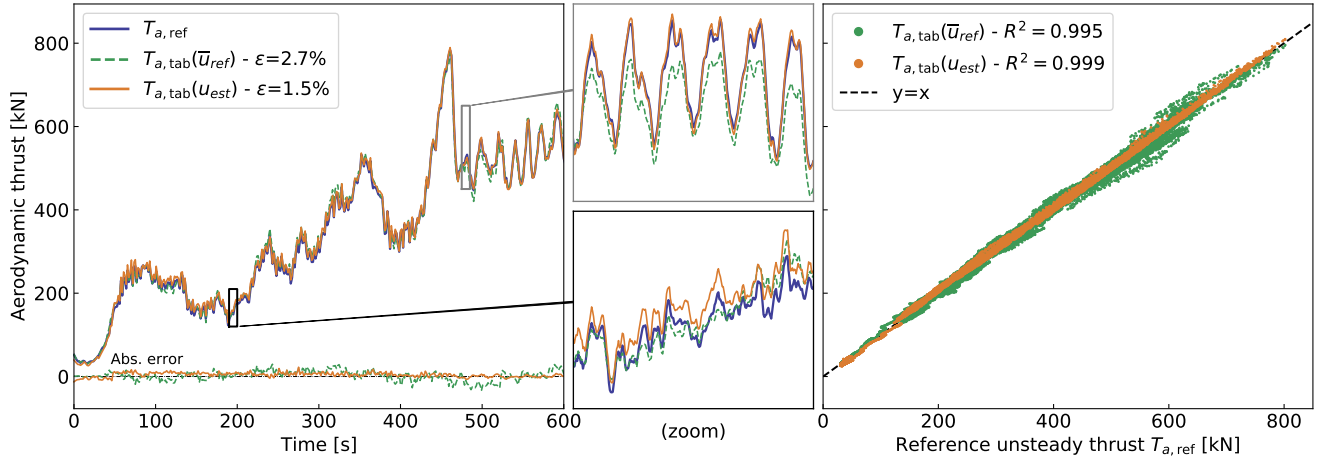


Figure 4. Comparison of aerodynamic thrusts: $T_{a,ref}$, obtained from a reference simulation; $T_{a,tab}(\bar{u}_{ref})$, obtained from tabulated C_T and the ~~rotor-averaged~~ rotor-averaged wind speed from the simulation; $T_{a,est} = T_{a,tab}(u_{est})$, obtained from the estimated wind speed. (Left:) Time series of thrust and absolute errors compared to the $T_{a,ref}$. (Right:) ~~Scatter-plot~~ Scatterplot of the tabulated thrust compared to the reference thrust.

285 3.3 Reduced model of the mechanical system

~~The 2-DOF~~ In this section, we compare the 2 DOF mechanical model presented in Section 2.1 ~~is here compared to the more~~ to the advanced OpenFAST model consisting of 16 DOF. As mentioned in Section 2.1, ~~we first improve~~ the generalized force ~~formulation~~ acting on q_t ~~can be further improved. The~~. We adopt the notations from Figure 2 ~~are adopted~~. The resulting force and moment at the ~~tower-top are written~~ tower top are written as \mathcal{F}_N and \mathcal{M}_N . The contribution of this load to the generalized
290 force is $\mathbf{f}_N = \mathbf{B}_N \cdot [\mathcal{F}_N; \mathcal{M}_N]$ where, according to the virtual work principle, \mathbf{B}_N is the velocity transformation matrix that provides the velocity of point N as a function of other DOFs. ~~More-DOF~~. Further details on this formalism are provided in Branlard (2019a). For the ~~single tower~~ single-tower DOF considered, the B -matrix consists of the end values of the shape function deflection and slope ~~-(i.e.,~~ $\mathbf{B}_N = [\Phi_{t,1}(L_t), 0, 0, 0, \nu_1, 0]$, where L_t is the length of the tower and $\nu_1 \triangleq \frac{d\Phi_{t,1}}{dz}(L_t)$. The shape functions are ~~assumed to be~~ normalized at their extremity ~~-(i.e.,~~ $\Phi_{t,i}(L_t) = 1$), so that the generalized force is:

$$295 \quad \mathbf{f}_N = \mathcal{F}_{x,N} + \nu_1 \mathcal{M}_{y,N} \quad (21)$$

~~The~~ We assumed that the main forces acting at the ~~tower-top are assumed to be~~ tower top are the aerodynamic thrust and the gravitational force from the rotor nacelle assembly (RNA) mass, M_{RNA} . ~~The loads are then obtained as:~~ We then obtain the loads as:

$$\mathcal{F}_{x,N} = T_a \cos(\alpha_y + \theta_{\text{tilt}}), \quad \mathcal{M}_{y,E} = T_a [x_{NR} \sin \theta_{\text{tilt}} + z_{NR} \cos \theta_{\text{tilt}}] + g M_{RNA} [x_{NG} \cos \alpha_y + z_{NG} \sin \alpha_y] \quad (22)$$

300 where, using Figure 2: θ_{tilt} is the tilt angle of the nacelle; NR is the vector from the ~~tower-top~~ tower top to the rotor center, where the thrust is assumed to act; NG is the vector from the ~~tower-top~~ tower top to the RNA center of mass; g is the acceleration of

gravity; and α_y is the y -rotation of the ~~tower-top due to the bending of the tower (see)~~ tower top induced by the tower bending. For a ~~single-tower mode~~ single-tower mode, $\alpha_y(t) = q_t(t)\nu_1$. The linearization of Equation 21 and Equation 22 for small values of q_t leads to:

$$f_N = q_t \{ -T_a \nu_1 \sin \theta_{\text{tilt}} + \nu_1^2 g M_{\text{RNA}} z_{NG} \} + (T_a \cos \theta_{\text{tilt}}) + T_a \nu_1 [x_{NR} \sin \theta_{\text{tilt}} + z_{NR} \cos \theta_{\text{tilt}}] + \nu_1 g M_{\text{RNA}} z_{NG} \quad (23)$$

where ~~the term in parenthesis~~ parentheses is the main contribution, which justifies the use of T_a in Equation 1; the term in curly brackets ~~is seen to act~~ acts as a stiffness term. The presence of T_a in this term ~~introduce~~ introduces an undesired coupling, and this term is kept on the ~~right-hand-side~~ right-hand side of Equation 1. It is noted that the vertical force, $\mathcal{F}_{z,N}$, contributes to the softening of the tower. The main softening effect attributed to the RNA mass is included in the stiffness matrix, as described in Branlard (2019a). The contribution of the thrust to the softening, ~~and as well as~~ additional contribution of quadratic velocity forces to the generalized force, are neglected.

~~The~~ We obtain the other elements of the 2D model ~~are obtained from~~ the OpenFAST input files. ~~The mass, stiffness and damping matrix of are obtained using~~ We use the YAMS library (Branlard, 2019a) ~~which~~—which can take as input an OpenFAST model, and thus use the same shape functions. ~~The functions~~—to obtain the mass, stiffness, and damping matrix of Equation 1. We use velocity transformation matrices to convert individual component matrices (e.g., blades, nacelle) into the global system matrices. The mass matrix thereby comprises the inertia terms from the tower and RNA. We tuned the damping of the 2 DOF model ~~was tuned based on using~~ simple “decay” simulations ~~to~~ to include the aerodynamic damping contribution. The simulation used for validation consists of a linear ramp of wind speed from 0 to 10 m s⁻¹ in the first 100 s, and a sudden drop to 6 ~~at 200s~~ m s⁻¹ at 200 s. The aerodynamic loads ~~and~~ the generator torque are extracted from the OpenFAST simulation and applied as external forces to the ~~reduced-order model~~. reduced-order model. Time series of tower-top positions, rotational speed ~~and tower bottom~~, and tower-bottom moments are compared in Figure 5. ~~The~~ We observe that the rotational speed is well captured, indicating that the rotational inertia is properly set, but also indicating that the ~~drive-train drivetrain~~ torsion does not have a strong impact for this simulation. The overall trend of the tower-top displacements is also well captured, though more differences are present ~~due to as a result of~~ missing contributions from additional blade and tower DOFs, ~~missing non-linearities-DOF, missing nonlinearities,~~ and quadratic velocity forces.

~~The~~ We use the method from Section 2.5 ~~is used~~ to estimate the bending moments along the tower from the tower-top displacement. The results shown on the right of Figure 5 indicate that the overall trends and load levels are well estimated, but some offsets are observed, which are a function of height. A contribution to the moment may be missing in the current model. This will be taken into consideration when ~~analysing~~ analyzing the results from the ~~KF~~ Kalman filter analysis.

330 4 Application to wind turbine tower loads estimation

Some of the individual models presented in Section 2 were briefly validated in Section 3. ~~The augmented KF~~ In this section, we use the augmented Kalman filter described in Section 2.3 ~~is now used~~, combining the different models together with the measurements. ~~The~~ We implement the state and output equations given in Equation 2 and Equation 3 ~~are implemented~~. The

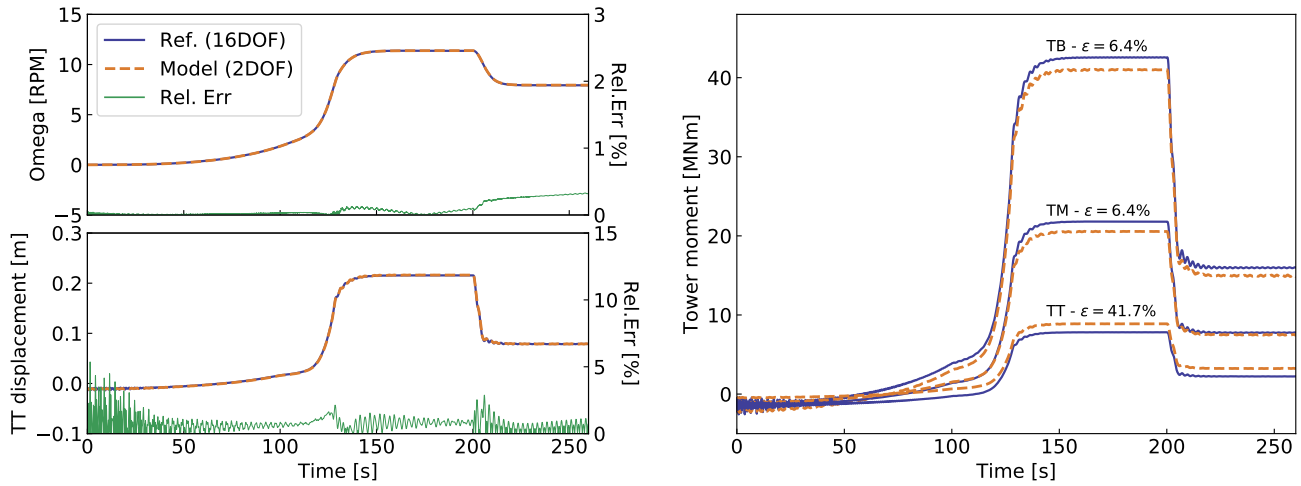


Figure 5. Simulation results using OpenFAST (16 DOF) and the reduced 2-DOF model. (Left): Rotational speed and tower-top (TT) displacements. (Right): Tower moments at three different heights: tower bottom (TB), tower middle (TM), and tower-top (TT). The TB moment is taken at 5% height above the ground and not exactly at the ground.

state equation is discretized. We discretize the state equation according to Equation 14 and provided to the KF algorithm.

Results from the KF-Kalman filter simulation, which combines a set of measurements with a model, will be referred to as “KF estimation.” The values used for the covariance matrices, P and Q and R , are discussed in Section 5.

4.1 Ideal cases without noise

The same simulation as the one presented in Section 3.1 is used, which extends from region 0 to region 3. The measurements sampled at 20 Hz are here directly taken directly from the OpenFAST simulation and not from a field experiment. This is obviously an ideal situation since no noise is because no noise or bias are present in the measurements. Further, the OpenFAST and KF-Kalman filter models are based on the same parameters, such as the mass and stiffness distribution. States-In Figure 6, we compare the states and tower loads estimated using the KF-model are compared-Kalman filter model with the simulation results in-. The signals are seen-observed to be well estimated by the KF-Kalman filter model over the entire range of operating regions. The error observed for the tower-bottom-tower-bottom moment is in the range of errors observed for the isolated mechanical system (Section 3.3).

A turbulent simulation is run, We ran a turbulent simulation at an average wind speed of 14 m s^{-1} with a turbulence intensity of 0.14, to illustrate the differences in the power spectral density of the signals. The results are given displayed in Figure 7 and commented further-on further. Frequencies that are not in the mechanical system (e.g. the second-FA, the second fore-aft [FA] mode and the DT-torsion-drivetrain torsion [DT]) are still “captured” by the estimator via the measurements. The rotational speed is directly observable by the KF-Kalman filter, so the signal is obviously well estimated. The thrust, is estimated based on the rotational speed, and thus exhibits similar frequencies as the rotational speed, which is not the case for

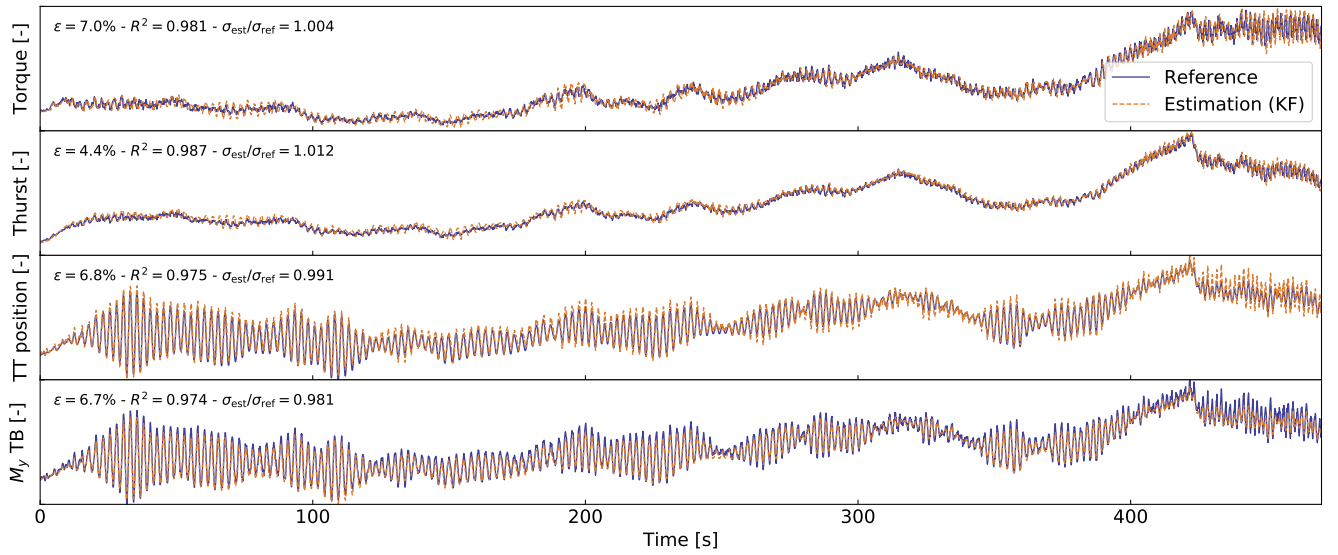


Figure 6. Comparison of signals simulated by OpenFAST (reference) compared with the ones estimated with the **KF-Kalman filter** model. From top to bottom, dimensionless time series of of: aerodynamic torque, aerodynamic thrust, tower-top displacement, **Fore-Aft tower-bottom** and **fore-aft tower-bottom** moment.

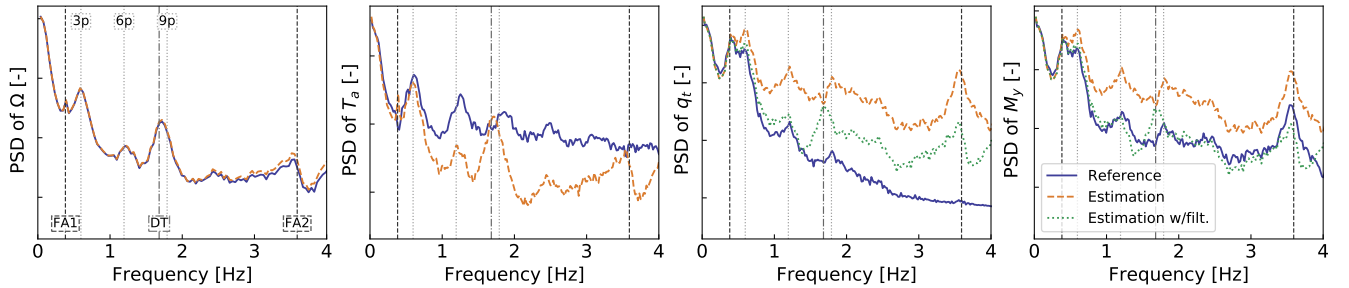


Figure 7. Power spectral density (PSD) of signals simulated by OpenFAST and estimated with the **KF-Kalman filter** model for a turbulent simulation at 14 m s^{-1} . From left to right: rotational speed, **Thrust**, **TT**-tower-top displacement, and **TB-FA**-tower-bottom fore-aft moment. Ticks on the y-axis represent two decades. The main system frequencies are marked with vertical lines: FA modes, **drivetrain torsion** (DT), and **multiple multiples** of the rotational frequency $p = 0.2$.

the reference thrust signal. The integration of the acceleration into the **TT**-tower-top position (q_t) shows a higher frequency content than the reference signal. The second FA frequency has a strong energy content in the estimated, q_t , signal. This frequency content comes from the acceleration signal, but it is not sufficiently captured and damped by the model, which does not represent the **second** mode. A moving average filter of period 1 s was introduced to reduce the high-frequency content of the acceleration. The results are **labelled**-labeled “Estimation w/filt.” on the figure. The analysis of the moment spectrum given on the right of Figure 7 indicates that the frequencies are well captured but the overall content at frequencies beyond the **first**

FA mode is too high. This is indicated by the values of the equivalent loads, which are respectively 20 MNm and 30 MNm for the reference and estimated signal, using a Wöhler slope of $m = 5$. The low-pass filter on the acceleration signal greatly improves the spectrum of M_y . The error in equivalent loads is further ~~quantifies in the next paragraph~~ quantified in Section 4.2.

4.2 Simulations with noise

The simulations presented in Section 4.1 used ~~as measurements~~ the simulated values from OpenFAST ~~as measurements~~. In this section, a Gaussian noise is added to each of the OpenFAST signals ~~in order~~ to account for measurement uncertainties. The noise level is taken ~~a as~~ 10% of the standard deviation of the signal simulated by OpenFAST. A noise level of 20% will be referred to as “Large noise”. ~~Simulations were performed with OpenFAST large noise.~~ We performed OpenFAST simulations for 10 wind speeds, with ~~six~~ 6 different turbulent seeds for each wind speed. ~~A noise level was applied~~ We applied a noise level to these simulation results ~~;~~ prior to feeding them to the ~~KF~~ Kalman filter estimator. Cases with or without applying the low-pass filter on the (noisy) acceleration input were tried. ~~Results~~ Figure 8 displays results for the error in equivalent load and standard deviation of the ~~TB~~ tower-bottom moment. The equivalent loads are estimated using a Wöhler slope of $m = 5$. As expected, the errors in standard deviation and equivalent loads follow similar trends. Errors without filtering

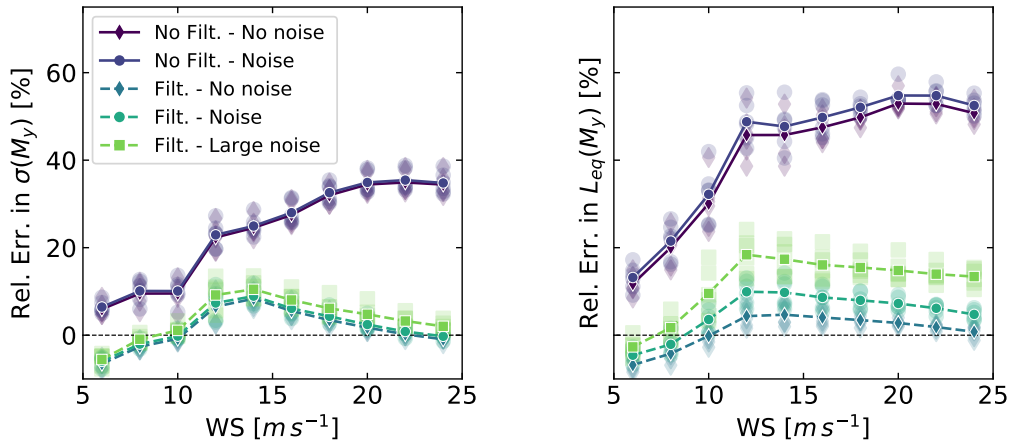


Figure 8. Comparison of the equivalent load and standard deviation of the ~~TB~~ tower-bottom moment as obtained by OpenFAST or as estimated from the ~~KF~~ Kalman filter estimator, for different noise levels and with or without a filter on the acceleration input. (Left): Error in standard deviation. (Right): Error in equivalent load. A positive value indicates that the estimator is overestimating. Individual markers indicate a simulation at a given wind speed and turbulence seed number. Lines indicate the mean values.

are ~~several fold~~ severalfold larger than when the acceleration is filtered. Without noise, the equivalent loads are estimated with $\pm 8\%$ error. The error increases with the noise level and the equivalent loads appear to be mostly overestimated. Further tuning of the filter and ~~of~~ the covariance matrices involved in the ~~KF~~ Kalman filter may reduce the error. Further discussions are provided in Section 5.

~~The framework is written~~ We wrote this framework in the noncompiled Python language ~~.The code was run and ran the code~~ on a single CPU. The average computational time for a 10 min period of measurements at 20 Hz was 37 s. Doubling the frequencies and the number of DOF would still keep the computational time ~~several-fold~~ ~~severalfold~~ smaller than real time. The expensive part of the algorithm is the ~~non-linear~~ ~~nonlinear~~ solve needed to find the optimal wind speed (Equation 16).

380 5 Discussion and future work

Measurements The results presented in the current study remained within the simulation realm. The accuracy of the method under uncertain conditions was partly quantified using various noise ~~models~~ ~~levels~~. ~~Yet, future~~ ~~Future~~ work will evaluate the model using field measurement data.

Model choices As mentioned in Section 2.3, a certain level of choice is present as to whether the loads are placed as an input or within the state vector. A consequence is that different load models may also be implemented, ~~for instance, such as~~ models of higher order than the one used in Equation 8. In the current study, a “random walk” force model was used for the torque, and the thrust was set as a dependent variable of the torque. ~~Yet~~ ~~However~~, these loads are functions of the axial inductions, which ~~typically are~~ ~~are~~ ~~typically~~ assumed to follow a ~~second-order~~ ~~second-order~~ model referred to as “dynamic wake.” A linearization of this model could be applied to the aerodynamic thrust and torque and potentially improve the performance prediction of the Kalman filter.

Nonlinearities and time invariance This study assumed a linear form of the equation of motion and that the system matrices were time-invariant. Despite this crude assumption, reasonable results were obtained. ~~Yet, further improvement~~ ~~Further~~ ~~improvements~~ are likely to be obtained if these assumptions are lifted. A simple approach would consist ~~in-of~~ updating the system matrices at some given interval based on a slow moving average on the wind speed or the tower-top position. ~~A more~~ ~~An~~ advanced method would use filtering methods that are adapted to ~~non-linear~~ ~~nonlinear~~ systems, such as extended Kalman filters or ~~partieles~~ ~~particle~~ filters. This approach would ~~yet, however~~, greatly increase the computational time. A shortcoming of the current approach is that the linear form of the equation was established “by hand”. ~~A more.~~ A systematic approach will be considered in the future ~~;~~ using the linearized form of the state matrices returned by OpenFAST, which would include aerodynamic damping directly.

Degrees of freedom and offshore application The general formalism presented in Section 2 can be applied to more degrees of freedom than the ~~2DOF-model-used~~ ~~÷~~ ~~2 DOF model used by~~ adding more shape function for the tower ~~;~~ and including side-side motion, yaw, tilt, shaft torsion, and blade motions. The results from the ~~2DOF~~ ~~2 DOF~~ model appeared encouraging enough to limit ourselves to this set, but future work will consider the inclusion of additional DOF. The extension of the method to offshore application could be done by adding extra degrees of freedom for the substructure, or ~~;~~ by using shape functions that

405 represent the entire support structure. The generalized force ~~due to~~ induced by the wave loading would need to be included. This force may be ~~modelled~~ modeled based on the wind speed, or assumed to be part of the model noise (see Section 2.3).

Model tuning Apart from the choices of degrees of freedom and model formulation, there remains a part of model tuning ; ~~through~~ through the choice of covariance matrices ; ~~and~~ ; and the potential filtering done on the measurements. As shown in Section 4.2, the filtering of the acceleration was ~~seen~~ observed to greatly improve the performance of the model. A time
410 constant of ~~1 s~~ 1 s was chosen empirically for the filter, but this value may need to be adapted for other applications. The choice of values used for the covariance matrices is usually the main source of criticism for ~~KF-based~~ Kalman-filter-based models. Indeed, these values have a strong influence on the results, and they are usually tuned empirically. For the current method to be successfully applied on various wind plants, an automatic tuning procedure is required. In the current study, the covariance matrices of the process were set automatically based on the value of the standard deviation of the simulated
415 signal at rated conditions. For the measurements, these values were divided by two. ~~It was~~ We found that this procedure ~~lead~~ led to satisfactory results. A sensitivity study should be considered in future work to give further insight on the procedure, ~~in particular~~ particularly if more states and measurements are used.

Wind speed estimation and standstill/idling condition The wind speed estimation model presented in Section 2.4 is limited to cases where the turbine is operating. Also, the accuracy of this model is crucial for the determination of the thrust, which in
420 ~~turns determine~~ turn determines the tower-top position and the tower loads. The nacelle velocity was ~~for instance~~ omitted in the current study and could be considered in future studies. ~~Wind speed estimation is a field in which the industry has a great expertise. Improvements~~ The industry has great expertise in wind speed estimation, and improvements on the algorithm would benefit the model presented in this ~~paper~~ article.

Airfoil performance The performance of the airfoils is a large source of uncertainty ~~which~~ that was not addressed. The thrust
425 was determined using tabulated C_T data, which may be significantly affected by the airfoil performance, which in turn are affected by blade erosion or other roughness sources ; ~~and~~ ; and additional uncertainty on the aerodynamic ~~modelling~~ modeling. Further improvement of the model is thus required to provide an accurate determination of the thrust that would account for such unknowns. Air density should also be considered for a correct account of the loading if a tabulated approach is used.

6 Conclusions

430 ~~The paper~~ In this article, we presented a general approach using Kalman filtering to estimate loads on a wind turbine, combining a mechanical model and a set of readily available measurements. ~~An open-source framework was established in hope to~~ We established an open-source framework in the hope that it will be further applied for real-time fatigue estimation of wind turbine loads, providing inspiration for a ~~digital twin~~ digital-twin concept. As an example, we presented the equations for a ~~2DOF~~ 2 DOF system of a wind turbine ~~were presented~~, and this system was used throughout the article. The study focused on the
435 estimation of tower bending moment, and in particular the associated damage equivalent load. Based on simulation results, we observed that the estimator was ~~seen to be~~ able to capture the damage equivalent loads with an accuracy ~~in~~ on the order of

10%. Future work will address the following points: use of field measurements, offshore application of the method, increased number of DOF, automatic covariance tuning, improved wind speed estimation in standstill, improved thrust determination in off-design conditions, and use of a linearized model obtained from an ~~aero-servo-elastic~~-aeroservoelastic tool.

440 *Author contributions.* The main concept behind this work originated from discussions between E. Branlard and C. Brown. E. Branlard performed the model derivations and wrote the article. C. Brown provided valuable feedback on the article and the methodology used. D. Giardina wrote a preliminary implementation of the model during his participation to a Science Undergraduate Laboratory Internship at NREL. E. Branlard extended the scripts to perform the analyses presented in this work.

Competing interests. No competing interests are present.

445 References

- Auger, F., Hilaiet, M., Guerrero, J. M., Monmasson, E., Orlowska-Kowalska, T., and Katsura, S.: Industrial Applications of the Kalman Filter: A Review, *IEEE Transactions on Industrial Electronics*, 60, 5458–5471, <https://doi.org/10.1109/TIE.2012.2236994>, 2013.
- Belloli, M.: Offshore floating wind turbines as sea state observers, *Journal of Physics: Conference Series*, 2019.
- Bertelè, M., Bottasso, C., and Cacciola, S.: Simultaneous estimation of wind shears and misalignments from rotor loads: formulation for
450 IPC-controlled wind turbines, *Journal of Physics: Conference Series*, 1037, 032 007, <https://doi.org/10.1088/1742-6596/1037/3/032007>, 2018.
- Bossanyi, E., Savini, B., Iribas, M., Hau, M., Fischer, B., Schlipf, D., van Engelen, T., Rossetti, M., and Carcangiu, C. E.: Advanced controller research for multi-MW wind turbines in the UPWIND project, *Wind Energy*, 15, 119–145, <https://doi.org/10.1002/we.523>, 2012.
- Bossanyi, E. A.: Individual Blade Pitch Control for Load Reduction, *Wind Energy*, 6, 119–128, <https://doi.org/10.1002/we.76>, 2003.
- 455 Bottasso, C. and Croce, A.: Cascading Kalman Observers of Structural Flexible and Wind States for Wind Turbine Control, Tech. rep., Dipartimento di Ingegneria Aerospaziale, Politecnico di Milano, Milano, Italy, Scientific Report DIA-SR 09-02, 2009.
- Bottasso, C., Croce, A., and Riboldi, C.: Spatial estimation of wind states from the aeroelastic response of a wind turbine, in: *The science of making torque from wind*, Heraklion, Crete, Greece, 2010.
- Boukhezzar, B. and Siguerdidjane, H.: Nonlinear Control of a Variable-Speed Wind Turbine Using a Two-Mass Model, *IEEE Transactions*
460 *on Energy Conversion*, 26, 149–162, <https://doi.org/10.1109/TEC.2010.2090155>, 2011.
- Bozkurt, T. G., Giebel, G., Poulsen, N. K., and Mirzaei, M.: Wind Speed Estimation and Parametrization of Wake Models for Downregulated Offshore Wind Farms within the scope of PossPOW Project, *Journal of Physics: Conference Series*, 524, <https://doi.org/10.1088/1742-6596/524/1/012156>, 2014.
- Branlard, E.: Flexible multibody dynamics using joint coordinates and the Rayleigh-Ritz approximation: The general framework behind and
465 beyond Flex, *Wind Energy*, 22, 877–893, <https://doi.org/10.1002/we.2327>, <https://doi.org/10.1002/we.2327>, 2019a.
- Branlard, E.: YAMS GitHub repository, <http://github.com/ebanlard/YAMS/>, 2019b.
- Dimitrov, N., Kelly, M. C., Vignaroli, A., and Berg, J.: From wind to loads: wind turbine site-specific load estimation with surrogate models trained on high-fidelity load databases, *Wind Energy Science*, 3, 767–790, <https://doi.org/10.5194/wes-3-767-2018>, 2018.
- Eftekhari Azam, S., Chatzi, E., and Papadimitriou, C.: A dual Kalman filter approach for state estimation via output-only acceleration
470 measurements, *Mechanical Systems and Signal Processing*, 60–61, 866–886, <https://doi.org/10.1016/j.ymssp.2015.02.001>, 2015.
- Evans, M., Han, T., and Shuchun, Z.: Development and validation of real time load estimator on Goldwind 6 MW wind turbine, *Journal of Physics: Conference Series*, 1037, 032 021, <https://doi.org/10.1088/1742-6596/1037/3/032021>, 2018.
- Grewal, M. S. and Andrews, A. P.: *Kalman Filtering: Theory and Practice Using Matlab*, John Wiley & Sons, Ltd,
475 <https://doi.org/10.1002/9781118984987>, 2014.
- Hafidi, G. and Chauvin, J.: Wind speed estimation for wind turbine control, in: *2012 IEEE International Conference on Control Applications*, pp. 1111–1117, <https://doi.org/10.1109/CCA.2012.6402654>, 2012.
- Hau, M.: Promising load estimation methodologies for wind turbine components, Upwind Deliverable 5.2, Tech. rep., Institut für Solare Energieversorgungstechnik (ISET), http://www.upwind.eu/pdf/D5.2_PromisingLoadEstimationMethodologies.pdf, 2008.

- 480 Iliopoulos, A., Shirzadeh, R., Weijtjens, W., Guillaume, P., Hemelrijck, D. V., and Devriendt, C.: A modal decomposition and expansion approach for prediction of dynamic responses on a monopile offshore wind turbine using a limited number of vibration sensors, *Mechanical Systems and Signal Processing*, 68-69, 84–104, <https://doi.org/https://doi.org/10.1016/j.ymssp.2015.07.016>, 2016.
- International Standard IEC, Workgroup 3: IEC 61400-3 Wind turbines: Design requirements for offshore wind turbines, IEC, 2005.
- Jacquelin, E., Bennani, A., and Hamelin, P.: Force reconstruction: analysis and regularization of a deconvolution problem, *Journal of Sound and Vibration*, 265, 81–107, [https://doi.org/https://doi.org/10.1016/S0022-460X\(02\)01441-4](https://doi.org/https://doi.org/10.1016/S0022-460X(02)01441-4), 2003.
- 485 Jonkman, J., Butterfield, S., Musial, W., and Scott, G.: Definition of a 5MW Reference Wind Turbine for Offshore System Development, Tech. Rep. NREL/TP-500-38060, National Renewable Energy Laboratory, 2009.
- Knudsen, T., Bak, T., and Soltani, M.: Prediction models for wind speed at turbine locations in a wind farm, *Wind Energy*, 14, 877–894, <https://doi.org/10.1002/we.491>, 2011.
- 490 Lourens, E., Reynders, E., Roeck, G. D., Degrande, G., and Lombaert, G.: An augmented Kalman filter for force identification in structural dynamics, *Mechanical Systems and Signal Processing*, 27, 446–460, 2012.
- Ma, C.-K. and Ho, C.-C.: An inverse method for the estimation of input forces acting on non-linear structural systems, *Journal of Sound and Vibration*, 275, 953–971, [https://doi.org/https://doi.org/10.1016/S0022-460X\(03\)00797-1](https://doi.org/https://doi.org/10.1016/S0022-460X(03)00797-1), 2004.
- Mendez Reyes, H., Kanev, S., Doekemeijer, B., and van Wingerden, J.-W.: Validation of a lookup-table approach to modeling turbine fatigue loads in wind farms under active wake control, *Wind Energy Science*, 4, 549–561, <https://doi.org/10.5194/wes-4-549-2019>, 2019.
- 495 OpenFAST: Open-source wind turbine simulation tool, available at <http://github.com/OpenFAST/OpenFAST/>, 2020.
- Østergaard, K. Z., Brath, P., and Stoustrup, J.: Estimation of effective wind speed, *Journal of Physics: Conference Series*, 75, 012082, <https://doi.org/10.1088/1742-6596/75/1/012082>, 2007.
- Schröder, L., Dimitrov, N. K., Verelst, D. R., and Sørensen, J. A.: Wind turbine site-specific load estimation using artificial neural networks calibrated by means of high-fidelity load simulations, *Journal of Physics: Conference Series*, 1037, 062027, <https://doi.org/10.1088/1742-6596/1037/6/062027>, 2018.
- 500 Selvam, K., Kanev, S., van Wingerden, J. W., van Engelen, T., and Verhaegen, M.: Feedback–feedforward individual pitch control for wind turbine load reduction, *International Journal of Robust and Nonlinear Control*, 19, 72–91, <https://doi.org/10.1002/rnc.1324>, 2009.
- Simley, E. and Pao, L.: Evaluation of a wind speed estimator for effective hub-height and shear components, *Wind Energy*, 19, 167–184, <https://doi.org/10.1002/we.1817>, 2016.
- 505 Soltani, M. N., Knudsen, T., Svenstrup, M., Wisniewski, R., Brath, P., Ortega, R., and Johnson, K.: Estimation of Rotor Effective Wind Speed: A Comparison, *IEEE Transactions on Control Systems Technology*, 21, 1155–1167, <https://doi.org/10.1109/TCST.2013.2260751>, 2013.
- Song, D., Yang, J., Dong, M., and Joo, Y. H.: Kalman filter-based wind speed estimation for wind turbine control, *International Journal of Control, Automation and Systems*, 15, 1089–1096, <https://doi.org/10.1007/s12555-016-0537-1>, 2017.
- 510 Zarchan, P. and Musoff, H.: Fundamentals of Kalman filtering: a practical approach, Fourth Edition, AIAA, Progress in astronautics and aeronautics, 2015.
- Ziegler, L., Smolka, U., Cosack, N., and Muskulus, M.: Brief communication: Structural monitoring for lifetime extension of offshore wind monopiles: can strain measurements at one level tell us everything?, *Wind Energy Science*, 2, 469–476, <https://doi.org/10.5194/wes-2-469-2017>, 2017.
- 515